

Density Functional Study of Size-Dependent Hydrogen Adsorption on Ag_nCr ($n = 1-12$) Clusters

Ngo Thi Lan, Nguyen Thi Mai,* Ngo Tuan Cuong, Phung Thi Hong Van, Duong Duc La, Nguyen Minh Tam, Son Tung Ngo, and Nguyen Thanh Tung*



Cite This: *ACS Omega* 2022, 7, 37379–37387



Read Online

ACCESS |



Metrics & More



Article Recommendations



Supporting Information

ABSTRACT: Increasing interest has been paid for hydrogen adsorption on atomically controlled nanoalloys due to their potential applications in catalytic processes and energy storage. In this work, we investigate the interaction of H_2 with small-sized Ag_nCr ($n = 1-12$) using density functional theory calculations. It is found that the cluster structures are preserved during the adsorption of H_2 either molecularly or dissociatively. $\text{Ag}_3\text{Cr}-\text{H}_2$, $\text{Ag}_6\text{Cr}-\text{H}_2$, and $\text{Ag}_9\text{Cr}-\text{H}_2$ clusters are identified to be relatively more stable from computed binding energies and second-order energy difference. The dissociation of adsorbed H_2 on Ag_2Cr , Ag_3Cr , Ag_6Cr , and Ag_7Cr clusters is favored both thermodynamically and kinetically. The dissociative adsorption is unlikely to occur because of a considerable energy barrier before reaching the final state for Ag_4Cr or due to energetic preferences for $n = 1, 5$, and $8-12$ species. Comprehensive analysis shows that the geometric structure of clusters, the relative electronegativity, and the coordination number of the Cr impurity play a decisive role in determining the preferred adsorption configuration.

INTRODUCTION

There is a fundamental interest in atomic clusters for the role they may play in understanding the complicated mechanism of hydrogen (H_2) adsorption on metal surfaces.¹ While hydrogen is considered as an infinite source of sustainable energy because of its environmental friendliness and high efficiency,^{2,3} looking for desirable hydrogen storage media is one of the important issues that currently limit its employment for daily energy supply. Solid-state storage of hydrogen is potentially a more compact and much safer approach⁴ that does not require high pressure and cryogenic temperature compared to compressed gas and liquefied one, respectively.⁵ In this regard, atomic clusters are often proposed as model solid-state systems for elucidating the formation of active sites on pure metal and alloy surfaces as well as their molecular-level interaction toward H_2 involved in hydrogen storage. For instance, the strong variation of H_2 reactivity patterns of neutral palladium clusters containing less than 25 atoms has been investigated by Fayet et al. using saturation measurements and gas-phase kinetic measurements.⁶ Following the pioneering work of Nonose and co-workers on the chemisorption of small clusters of aluminum with hydrogen,⁷ the reaction mechanism of charged and neutral aluminum clusters and their doped species with H_2 has been later explored in terms of both theoretical and experimental approaches.⁸⁻¹⁴ The geometric and electronic structures of hydrogenated scandium, titanium, and zirconium clusters have been examined by Kumar et al. and Sheng et al.^{15,16} Swart and co-workers investigated the H_2 adsorption on 3d transition metal clusters in combined infrared spectroscopy and density functional study.¹⁷ Density functional theory (DFT) calculations have been performed to understand the adsorption and dissociation pathway of H_2 molecule on magnesium doped with transition metal

atoms.¹⁸⁻²⁰ The bonding characters and adsorption energies of H_2 molecules on pure and decorated boron fullerenes/spheres have been extensively studied due to their potential for hydrogen storage media.²¹⁻²⁹

While materials made of lightweight elements are often considered for mobile hydrogen storage applications, various noble-metal based clusters and their alloy species have been envisaged for stationary hydrogen storage purposes at either production or end-use site.³⁰ For instance, the interaction nature and the favorable bonding type between a gold cluster and H atoms have been theoretically examined by Phala et al.³¹ Photoelectron spectroscopy and ion trap mass spectrometry performed by Buckart et al. and Lang et al., respectively, indicated that even-sized cationic gold clusters adsorbed molecular oxygen, while anionic ones do not.^{32,33} Hydrogen molecule adsorption on Au_nPt ($n = 1-12$) clusters has been investigated and compared with corresponding pure clusters by Fang and Kuang.³⁴ The effect of hydrogen adsorption on the structure and electronic properties of gold clusters and their small alkali auride species has been evaluated and discussed by Mondal et al. and Li et al., respectively.^{35,36} Silver clusters appear as an attractive alternative in terms of commonness and cost-effectiveness compared to gold or platinum counterparts. Small neutral, anionic, and cationic silver cluster hydrides Ag_nH and anionic HAg_nH ($n = 1-7$) studied using the density functional method have shown that the adsorption site is

Received: June 30, 2022

Accepted: September 23, 2022

Published: October 3, 2022



Table 1. Calculated Binding Energies for AgH and CrH Dimers Using Different Functions in Conjunction with cc-pVDZ-pp for Ag Atoms, cc-pVDZ for Cr Atoms, and LanL2DZ/SDD for H One^a

	PW91		PBE		BP86		experiment ⁴⁵
	LanL2DZ	SDD	LanL2DZ	SDD	LanL2DZ	SDD	
AgH	2.37	2.37	2.36	2.35	2.40	2.49	2.6 ± 0.08
CrH	2.16	2.23	2.12	2.20	2.31	2.39	2.9 ± 0.52

^aThe corresponding experimental values from ref 45 are also included for comparison.

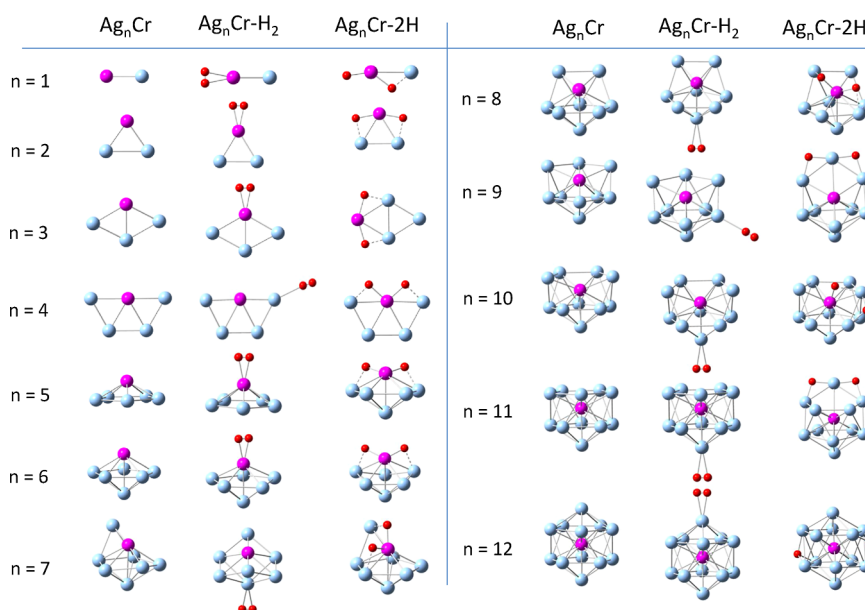


Figure 1. (Color online) Optimized structures of Ag_nCr , $\text{Ag}_n\text{Cr-H}_2$, and $\text{Ag}_n\text{Cr-2H}$ clusters ($n = 1-12$). The light blue, violet, and red spheres represent Ag, Cr, and H atoms, respectively.

strongly governed by the cluster charge and size.^{37,38} Manzoor and Pal have shown that the reactivity and catalytic properties of silver clusters with a chemisorbed hydrogen atom are greatly enhanced compared with those of the bare species.³⁹ Lately, Perera and co-workers have demonstrated that the H_2 adsorption behavior of silver clusters is not only altered when being downsized but can also be fundamentally tailored by proper doping.⁴⁰ Being motivated by the search for potential hydrogen storage nanostructured materials, this study aims to theoretically explore the important role of the chromium dopant in H_2 adsorption and dissociation on small silver clusters. The structures, relative stability, bonding characters, electronic properties, and adsorption energies of Ag_nCr ($n = 1-12$) are calculated, analyzed, and discussed to evaluate the most potential system within the H_2 adsorption limit.

COMPUTATIONAL METHOD

In the present work, the search for ground-state geometries of all structures and hydrogen adsorption was conducted by the DFT calculations implemented in the Gaussian 09 package.^{41,42} For all calculations, guessing structures were first optimized using the BP86 functional in conjunction with cc-pVDZ-pp for Ag atoms, cc-pVDZ for Cr atoms, and SDD for H ones. Isomers with relative energies less than 1.5 eV were selected for recalculating single-point energies at the same functional but combined with larger basis sets, cc-pVTZ-pp and cc-pVTZ for Ag and Cr atoms, respectively. This approach is a good compromise between accuracy and computational

effort and reliable for transition metal-doped silver species.^{43,44} The reliability and accuracy of our calculations are further tested by examining the binding energy of AgH and CrH dimers using several Lan functions (PW91, PBE, and BP86) in conjunction with LanL2DZ and SDD for H. The results are summarized in Table 1. It is obvious that the computed binding energies of AgH and CrH with BP86/SDD (2.49 and 2.39 eV) are closest to the experiment values of 2.6 ± 0.08 and 2.9 ± 0.52 ,⁴⁵ respectively. Based on these benchmark data, we are confident that the used computational approach is suitable to predict the interaction between hydrogen and Ag_nCr clusters.

A large number of Ag_nCrH_2 structures were constructed using the stochastic genetic algorithm⁴⁶ as well as manually built based on placing a hydrogen molecule or two hydrogen atoms on many different adsorption positions and orientations of the Ag_nCr cluster.⁴³ The vibrational frequencies were calculated and examined to ensure the structure's existence at the minima on the potential energy surface. Different possible spin multiplicities were considered for each geometry to ensure the robustness of the ground-state optimization process. The transition state (TS) geometries are determined by using the quadratic synchronous transit method⁴⁷ through scanning relaxed potential energy surface with proper internal coordinates. The intermediates are connected to each TS by tracing the intrinsic reaction coordinate.⁴⁸ Vibrational frequency calculations are carried out to make sure each TS has only one imaginary frequency, while the intermediate does not.

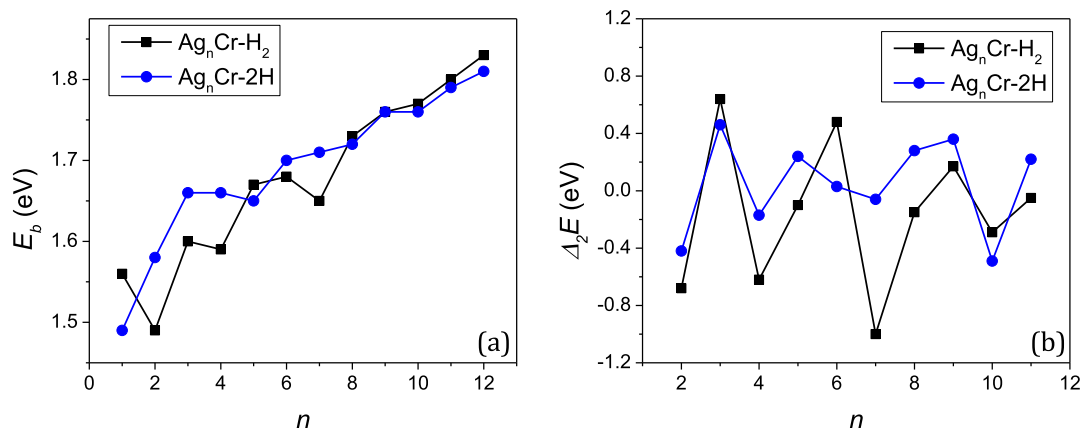


Figure 2. (Color online) (a) Binding energy per atom (E_b) and (b) second-order energy difference (Δ_2E) of Ag_nCr-H_2 and Ag_nCr-2H clusters.

RESULTS AND DISCUSSION

Optimized Geometrical Structures. The first aim of our computational efforts is to predict plausible ground-state geometries of hydrogen adsorption on Ag_nCr clusters that can be useful in guiding further experiments. For this purpose, a large number of different geometrical and spin isomers for each stoichiometry is calculated. Figure 1 presents the optimized structures for both molecular (Ag_nCr-H_2) and dissociative (Ag_nCr-2H) adsorption configurations with $n = 1-12$. The lowest energy structures for bare Ag_nCr clusters are also recalculated for validation.⁴³ Other low-lying isomers for Ag_nCr-H_2 and Ag_nCr-2H clusters are shown in the Supporting Information.⁴⁹

It can be seen that small bare Ag_nCr clusters favor the planar motif with the vertex Cr atom until $n = 5$, where the cluster undergoes a 2D–3D transition with five silver atoms binding to the Cr atom to form a pentagonal pyramid structure. The growth sequence of larger species prefers a build-up of the second pentagonal pyramid and finally forms the icosahedral structure $Ag_{12}Cr$ with the central Cr atom. As the number of Ag atoms increases, the preferred position of the Cr atom changes from edge sites to partially and then completely encapsulated ones.

The adsorption of molecular hydrogen does not alter the structures of bare Ag_nCr clusters. The calculations reveal the two most stable kinds of adsorption sites: (i) to the Cr atom for $n = 1-3, 5$, and 6 and (ii) to one of the surface Ag host atoms for other sizes. The adsorption on Cr–Ag and Ag–Ag bridging sites is found considerably less stable. It is interesting when putting this result together with previous ones for transition metal-doped species.^{12–14,18} The most favored adsorption position is often on the surface impurity site. For instance, the energetically preferred adsorption site for Al_nCr ($n = 1-13$) clusters is on the Cr top site.¹² The H_2 molecule also likely goes for the Co dopant top site in Mg_nCo clusters ($n = 1-10$) and one of the Rh atoms in Al_nRh_2 ($n = 1-9$).^{14,18} A proper combination of the cluster size and composition can induce the H_2 adsorption on one of the surface Ag atoms or on Ag–Ag bridging positions, where the transition metal impurity can be encapsulated or coordination-saturated.¹³ Our finding for Ag_nCr clusters with $n = 7-12$ is in line with this argument. It should be noticed that H_2 molecule adsorbed in the planar Ag_4Cr to a vertex Ag atom instead of the surface Cr atom and this will be discussed later.

If the clusters started absorbing H_2 as a molecule, the following dissociation of H_2 may trigger a structural transformation.^{12,13,18} Nevertheless, the stable Ag_nCr structures are almost preserved when the adsorbed H_2 dissociates, except for slightly distorted Ag_9Cr-2H and $Ag_{11}Cr-2H$. In particular, as shown in Figure 1, one Ag atom is moderately pulled out of the three-member and five-member Ag string in Ag_9Cr and $Ag_{11}Cr$, respectively, after dissociating H_2 . The dissociative adsorption behavior of H_2 can be generalized into two regions depending on the position of the Cr atom: Individual hydrogen atoms favorably bind to the bridging Cr–Ag sites for the surface Cr atom ($n = 1-8$, and 10) and to the bridging Ag–Ag sites for the encapsulated Cr atom ($n = 9, 11$, and 12). For $AgCr-2H$, one H atom binds to the Cr–Ag bridging site, while the other one prefers the top Cr site.

It is noticeable that the hydrogen molecule favors forming a bond to the surface Cr atom (with $n = 1-6$, except $n = 4$) rather than to an Ag atom. Another striking feature is that the individual H atoms prefer the bridging position between the surface Cr atom (with $n = 1-8$) and one Ag atom. The most plausible explanation for preferred bonds of hydrogen to the surface Cr atom is their electronegativity χ . In the Pauling scale, χ_{Cr} is 1.6 and χ_{Ag} is 1.9, while that of H is 2.1. Since the bonding usually requires electron transfers, the bond between a lowest- χ atom (Cr) and a highest- χ atom (H) is favorable. While the hydrogen adsorption site is evidently governed by the electronegativity difference, the atomic coordination number N also plays a vital role. It is known that the atomic coordination number of a surface atom is inversely proportional to its adsorption energy for small molecules.⁵⁰ That means the less the coordination number of an atom, the more favorable is adsorption on it. With this picture in mind, one might be able to understand the case of Ag_4Cr-H_2 , where a hydrogen molecule is adsorbed to a vertex Ag atom ($N_{Ag} = 2$) instead of the surface Cr impurity ($N_{Cr} = 4$). The same argument can be drawn for Ag_9Cr-2H , where the H atoms prefer bridging positions between two vertex Ag atoms rather than Cr–Ag ones. Very similar results were reported for the hydrogen adsorption on Al_nRh^+ , $Al_nRh_2^+$, and Al_nCr clusters,^{12–14} where the low coordination of the impurity atom (Rh and Cr) is an influential factor for determining the favorable adsorption site. This could help us decipher how the interplay between the electronegativity and the number of coordination takes the lead in deciding the preferred adsorption site of hydrogen on Ag_nCr clusters.

Table 2. Calculated Average Binding Energies Per Atom [E_b (eV)], Second-Order Energy Differences [Δ_2E (eV)], Adsorption Energies [E_{ad} (eV)], and H–H Bond Length [d_{H-H} (Å)] for Molecular and Dissociate Adsorption of Hydrogen on Ag_nCr Clusters^a

<i>n</i>	E_b (eV)		Δ_2E (eV)		E_{ad} (eV)		d_{H-H} (Å)	
	Ag_nCr-H_2	Ag_nCr-2H	Ag_nCr-H_2	Ag_nCr-2H	Ag_nCr-H_2	Ag_nCr-2H	Ag_nCr-H_2	Ag_nCr-2H
1	1.56	1.49			0.49	0.19	0.78	3.25
2	1.49	1.58	−0.68	−0.42	0.60 (1.05)	1.04 (1.36)	0.82	3.57
3	1.60	1.66	0.64	0.46	0.77 (0.52)	1.13 (0.85)	0.79	3.63
4	1.59	1.66	−0.62	−0.17	0.48 (0.30)	0.96 (0.69)	0.76	2.67
5	1.67	1.65	−0.10	0.24	0.77	0.63	0.79	2.68
6	1.68	1.70	0.48	0.03	0.72 (0.52)	0.86 (0.57)	0.79	2.93
7	1.65	1.71	−1.00	−0.06	0.05 (0.20)	0.65 (0.33)	0.77	2.38
8	1.73	1.72	−0.15	0.28	0.67	0.56	0.76	2.72
9	1.76	1.76	0.17	0.36	0.23	0.20	0.76	3.51
10	1.77	1.76	−0.29	−0.49	0.23	0.06	0.77	3.20
11	1.80	1.79	−0.05	0.22	0.24	0.15	0.77	3.52
12	1.83	1.81			0.25	−0.04	0.77	3.97

^aThe values in brackets are adsorption energies (ΔG_{298K} in eV) accounting for entropic effects.

Relative Stability. The stability is usually considered as an important parameter to gain insight into the size-dependent stable patterns and possibly understand the reaction direction of absorbed complexes. In this regard, the average binding energy per atom (E_b) can be used as a reliable measure of the cluster's relative stability. Generally, E_b is defined as the average gained energy per atom during the formation of a cluster from all free constituent atoms. The average binding energy per atom for both molecular Ag_nCr-H_2 and dissociative adsorption Ag_nCr-2H can be expressed as follows

$$E_b(Ag_nCr - H_2) = \frac{1}{n+3} [nE(Ag) + E(Cr) + 2E(H) - E(Ag_nCr - H_2)] \quad (1)$$

$$E_b(Ag_nCr - 2H) = \frac{1}{n+3} [nE(Ag) + E(Cr) + 2E(H) - E(Ag_nCr - 2H)] \quad (2)$$

where E is the total energy of the cluster or atom. Figure 2a presents the variation of E_b for both Ag_nCr-H_2 and Ag_nCr-2H species versus the cluster size. Their corresponding values are listed in Table 2. At the first glance, it is seen that E_b values roughly increase (1.50–1.83 eV) with the size for both species. It should be noted that the E_b values for bare Ag_nCr clusters are considerably smaller for $n = 1-6$ (from 0.75 to 1.40 eV) and slightly lesser for $n = 7-12$ (from 1.48 to 1.73 eV).⁴³ This implies that after releasing hydrogen, the clusters with $n = 7-12$ will secure their stability better than those with $n = 1-6$. An interesting feature is the higher E_b values of Ag_nCr-H_2 clusters compared to the corresponding ones of Ag_nCr-2H counterparts at $n = 1, 5,$ and $8-12$, suggesting that the molecular adsorption seems to be more favorable at these sizes. It is also worth noting that there are local maxima in the average binding energy graph at $n = 3, 6,$ and 9 for Ag_nCr-H_2 and $n = 3$ and 9 for Ag_nCr-2H , agreeing well with the relatively high stability of bare $Ag_3Cr, Ag_6Cr,$ and Ag_9Cr clusters.⁴³

The relative stability of Ag_nCr-H_2 and Ag_nCr-2H among neighboring sizes is further analyzed using the calculated second-order energy difference (Δ_2E). The second-order energy difference is the energy difference between a cluster

and its immediate neighboring sizes and can be obtained as follows

$$\begin{aligned} \Delta_2E(Ag_nCr - H_2) &= E(Ag_{n-1}Cr - H_2) + E(Ag_{n+1}Cr - H_2) \\ &\quad - 2E(Ag_nCr - H_2) \end{aligned} \quad (3)$$

$$\begin{aligned} \Delta_2E(Ag_nCr - 2H) &= E(Ag_{n-1}Cr - 2H) + E(Ag_{n+1}Cr - 2H) \\ &\quad - 2E(Ag_nCr - 2H) \end{aligned} \quad (4)$$

where E is the total energy of the cluster or atom. Figure 2b presents the variation of Δ_2E as a function of the cluster size for both molecular and dissociative adsorption configurations. Their calculated values are also listed in Table 2. Two conspicuous maxima are found at $n = 3$ and 9 for both Ag_nCr-H_2 and Ag_nCr-2H species, indicating their enhanced stability compared with their neighbors. A plausible explanation can be attributed to the stability inherited from bare Ag_3Cr and Ag_9Cr , where the joint orbitals between the dopant 3d electrons and the electrons in the silver stabilize and enhance the bonding between silver and chromium.⁴³ Two distinct peaks are observed for Ag_5Cr-2H and Ag_6Cr-H_2 , suggesting that they are relatively more stable among their neighbors. While the enhanced stability of Ag_6Cr-H_2 is in line with the calculated average binding energy graph in Figure 2a, E_b of Ag_5Cr-2H is less noticeable. The increasing trend is seen at $n = 11$ for both hydrogenated configurations as found for bare Ag_nCr species, but no comment can be made due to the limitation of studied sizes.

Hydrogen Adsorption Process. The accumulation of small molecules on a surface is known as the adsorption process. Based on the accumulating nature, the adsorption can be generally classified as the physisorption (molecular adsorption) characterized by weak van der Waals forces and the chemisorption (dissociative adsorption) featured by chemical bonding. The adsorption process can be influenced by various parameters, for example, the details of the host species involved, the adsorption type, and the energy barrier between the hydrogen molecule and the surface. In this regard,

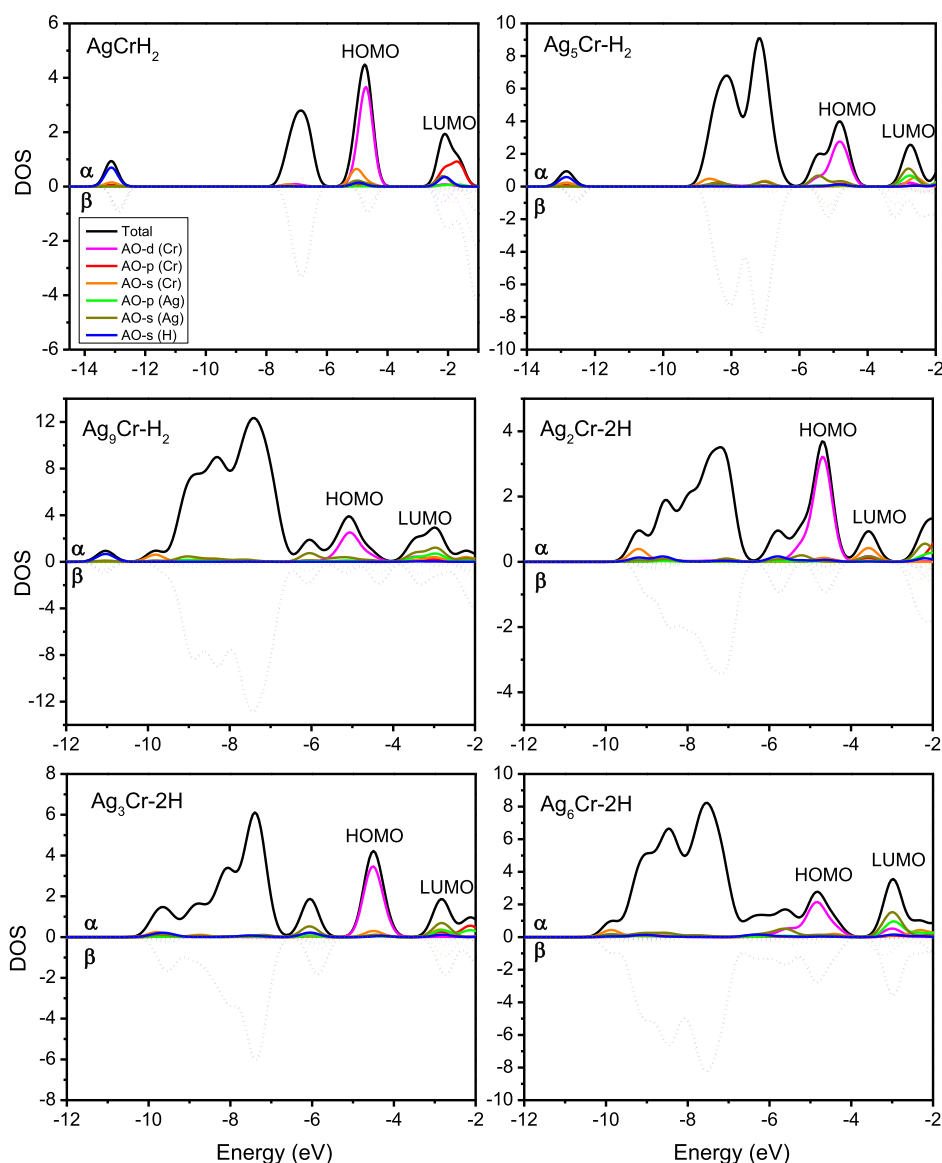


Figure 3. (Color online) DOS of AgCr-H_2 , $\text{Ag}_5\text{Cr-H}_2$, and $\text{Ag}_8\text{Cr-H}_2$ clusters. HOMO and LUMO stand for highest occupied molecular orbitals and lowest unoccupied molecular orbitals, respectively.

the adhesion of a single hydrogen molecule on a well-defined bimetallic nanocluster is exciting to be explored as an ideal model for fundamental insights into the adsorption process. To investigate the adsorption process of H_2 on the Ag_nCr clusters ($n = 1-12$), the adsorption energy and the H–H bond length for both molecular adsorption and dissociative adsorption configurations are therefore calculated as follows

$$E_{\text{ad}}(\text{Ag}_n\text{Cr} - \text{H}_2) = E(\text{Ag}_n\text{Cr}) + E(\text{H}_2) - E(\text{Ag}_n\text{Cr} - \text{H}_2) \quad (5)$$

$$E_{\text{ad}}(\text{Ag}_n\text{Cr} - 2\text{H}) = E(\text{Ag}_n\text{Cr}) + E(\text{H}_2) - E(\text{Ag}_n\text{Cr} - 2\text{H}) \quad (6)$$

The results are also listed in Table 2. The H–H bond length $d_{\text{H-H}}$ is found considerably stretched (from 0.79 to 0.82 Å) for $\text{Ag}_n\text{Cr-H}_2$ clusters with $n = 2, 3, 5$, and 6 compared to that of the isolated H_2 (0.75 Å). The elongated H–H distance indicates that H_2 seems to be activated after adsorbing on these

Ag_nCr surfaces. As can be seen from eqs 5 and 6, the adsorption energy is equal to the total energy difference between the reactants ($\text{H}_2 + \text{Ag}_n\text{Cr}$) and the product ($\text{Ag}_n\text{Cr-H}_2$ or $\text{Ag}_n\text{Cr-2H}$), representing the smallest energy required for the adsorbate to be desorbed from the surface. Except for $\text{Ag}_{12}\text{Cr-2H}$, all computed E_{ads} energies take positive values. In addition, we found that the E_{ads} varies from 0.05 to 0.77 eV for $\text{Ag}_n\text{Cr-H}_2$ clusters and from -0.04 to 1.13 eV for $\text{Ag}_n\text{Cr-2H}$, but the general tendency is to decrease with increasing size. The lowering adsorption barrier could be attributed to the enhancing trend of average binding energies as n goes from 1 to 12. It is also interesting to compare the molecular adsorption energy and the dissociative adsorption energy because of the same reactants. The computed E_{ads} values for $\text{Ag}_n\text{Cr-2H}$ are higher than those for $\text{Ag}_n\text{Cr-H}_2$ at $n = 2-4, 6$, and 7, meaning that dissociating the adsorbed H_2 molecule on these species is an exothermic process and thermodynamically preferred. Bearing this picture in mind, one can imagine that, in other words, the molecular adsorption likely occurs for Ag_nCr with $n = 1, 5$, and 8–12. Meanwhile, after approaching

the surface of Ag_nCr ($n = 2-4, 6, \text{ and } 7$), H_2 undergoes molecular adsorption and is eventually dissociated to form strong bonds with the cluster. Of course, the dissociation of adsorbed H_2 also depends on the overcoming of the activation barrier to take place, and that possibility will be discussed later.

In order to understand the binding nature of adsorbed hydrogen molecules on Ag_nCr clusters, the densities of electronic states (DOS) are computed and plotted in Figure 3 for selected thermodynamically preferred configurations. The results for other species are provided in the Supporting Information.⁴⁹ As can be seen, all partial and total densities of states are presented in each graph, while the solid and dashed lines correspond to states with spin-up (α) and spin-down (β) orientations. For physisorption-feasible species $\text{AgCr}-\text{H}_2$, $\text{Ag}_5\text{Cr}-\text{H}_2$, and $\text{Ag}_9\text{Cr}-\text{H}_2$ in Figure 4, most of the electronic states associated with the adsorbed hydrogen are located at the low-energy side (-13 and -12 eV) and well separated from the cluster states (above -8 eV). Since there is no overlap between hydrogen states and cluster ones, it can be confirmed that the chemical bonding makes a relatively small or almost zero contribution to the binding nature of hydrogen and these species. A plausible source of bonding for H_2 to these clusters can be the electrostatic interaction between charge-polarized hydrogen and metal atoms. The electronic states associated with hydrogen in $\text{Ag}_2\text{Cr}-2\text{H}$, $\text{Ag}_3\text{Cr}-2\text{H}$, and $\text{Ag}_6\text{Cr}-2\text{H}$ show the opposite picture. In particular, the hydrogen electronic states entirely diffuse to the high-energy side (above -10 eV) to make a strong hybridization with the cluster states. The pure character of H_2 lying on the low-energy side is no longer observed as expected. It is worth mentioning that in all cases, the HOMO states are mainly contributed by 3d-Cr orbitals. Since the bonding usually requires electron transfers, this observation supports our above-mentioned argument why the H_2 adsorption prefers the surface Cr site.

To gain more insight into the dissociative process, possible reaction pathways connecting the reactants and the final configuration for the single H_2 adsorption and dissociation on Ag_2Cr , Ag_3Cr , and Ag_6Cr clusters are calculated and presented in Figure 4. The relative Gibbs free energies ($\Delta G_{298\text{K}}$ in eV) are given with respect to the initial reactants ($\text{Ag}_n\text{Cr} + \text{H}_2$). The corresponding ones for Ag_4Cr and Ag_7Cr clusters as well as their intrinsic reaction coordinates are provided in the Supporting Information.⁴⁹ The activation barrier for the dissociation is determined by the total energy difference between the reactants and the TS. According to the snapshots along the dissociation path in Figure 4, the structures of Ag_2Cr , Ag_3Cr , and Ag_6Cr clusters are preserved during the H_2 adsorption and dissociation. The H_2 dissociation takes place on top of the Cr atom when two H atoms get activated and separated. In their final configurations, two H atoms form bridges between the Cr atom and the nearest Ag atoms. For the interaction of H_2 with Ag_2Cr (see Figure 4a), it is found that all TSs associated with the dissociation process are considerably lower in energy (0.87 and 1.07 eV for TS_1 and TS_2 , respectively) compared with the reactants. Although there are submerged barriers required to overcome TS_1 and TS_2 , their computed values of only 0.18 and 0.05 eV with respect to connecting intermediates, respectively, are minor and negligible. The final configuration with dissociated hydrogen $\text{Ag}-2\text{Cr}-2\text{H}$ is hence thermodynamically and kinetically preferred.

Similar pictures can be applied for species with $n = 3, 6, \text{ and } 7$. As seen in Figures 4b,c, and S9 in the Supporting Information, the TSs and intermediates involved in the (not

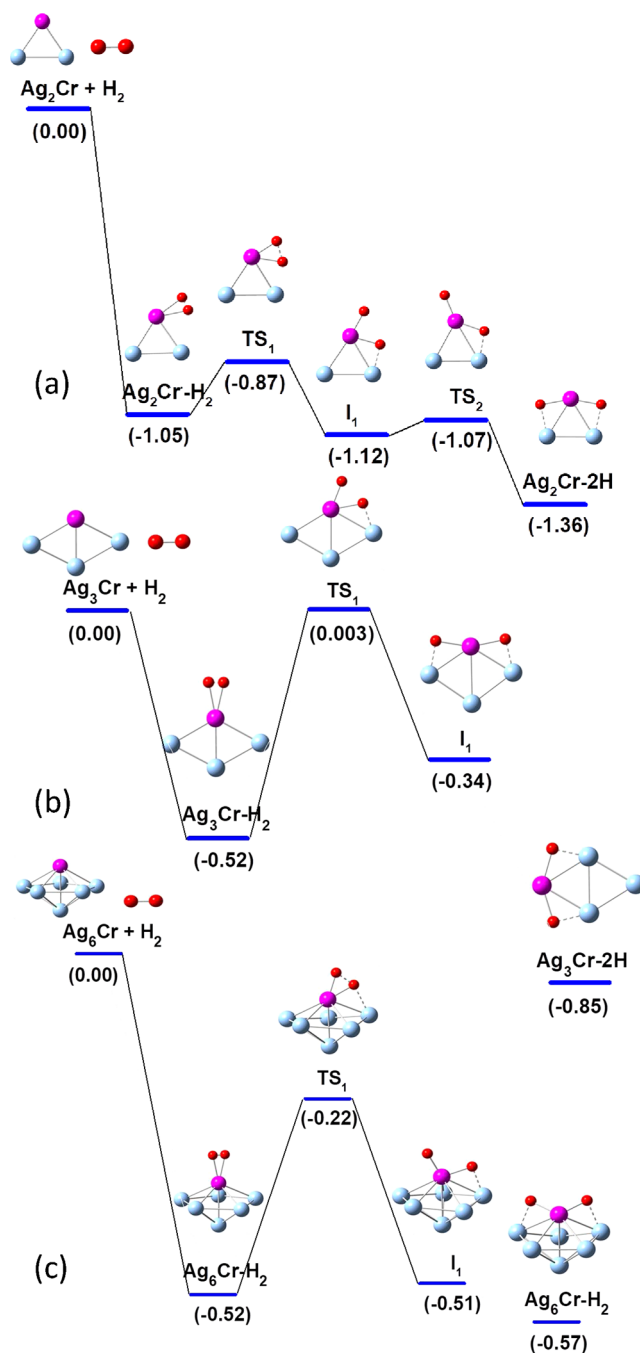


Figure 4. (Color online) Calculated reaction pathways and relative Gibbs free energies ($\Delta G_{298\text{K}}$ in eV) for the molecular and dissociative adsorption of H_2 on (a) Ag_2Cr , (b) Ag_3Cr , and (c) Ag_6Cr . The intermediates and TSs are denoted as I_1 and TS_i . Light blue, violet, and red spheres represent Ag, Cr, and H atoms, respectively.

the entire process) dissociation of H_2 on Ag_3Cr , Ag_6Cr , and Ag_7Cr clusters and their corresponding relative energies are plotted. Their incompleteness of reaction pathways (for Ag_3Cr and Ag_6Cr) might skip other (possibly even higher) barriers before reaching the final state with dissociated H_2 , but the presented energy profiles could be sufficient to learn about possible kinetic traps of hydrogen relative to activating, intermediate, and separating states. In particular, the dissociation of molecularly adsorbed H_2 on Ag_3Cr needs to subdue a minor energy barrier of 0.523 eV for TS_1 (+0.003 eV) with respect to the connecting intermediate (-0.520 eV). For

H₂ on Ag₆Cr, a submerged barrier of 0.30 eV for TS₁ (−0.22 eV) with respect to the connecting intermediate (−0.52 eV) is also encountered. Also, for H₂ on Ag₇Cr, two submerged barriers of 0.06 eV for TS₁ (−0.14 eV) with respect to the connecting intermediate (−0.20 eV) and 0.01 eV for TS₂ (−0.24 eV) regarding the connecting intermediate (−0.25 eV) must be taken into account. In addition, as above discussed, Ag₃Cr−2H, Ag₆Cr−2H, and Ag₇Cr−2H isomers are found more thermodynamically favorable than their counterparts with molecularly adsorbed H₂. Therefore, the current results support the dissociative adsorption of H₂ on Ag₃Cr, Ag₆Cr, and Ag₇Cr clusters. Ag₄Cr is a different case. Although the final configuration with dissociative H₂ on Ag₄Cr is considerably lower in Gibbs free energy (−0.69 eV) with regard to the entrance channel, the dissociation process of molecularly adsorbed H₂ on Ag₄Cr suffers from an energy barrier of 1.38 eV (TS₁) as shown in Figure S4 in the [Supporting Information](#).⁴⁹ Thus, it is safe to state that the adsorption of a hydrogen molecule is preferable on Ag₄Cr, but its dissociation process is unlikely to occur without external stimuli.

CONCLUSIONS

In summary, we have investigated the interaction between H₂ and Ag_{*n*}Cr clusters (*n* = 1–12) using DFT calculations. The strongly size-dependent structure, stability, and reactivity toward H₂ were observed. The calculated results imply that the geometric structure of clusters, the relative electronegativity χ , and the coordination number *N* of the Cr impurity play a decisive role in determining the adsorption configuration. In particular, the Cr atom prefers surface sites for *n* = 1–6 and encapsulated ones for *n* = 7–12. Since χ_{Cr} is smaller than χ_{Ag} , the most favored adsorption position of hydrogen is often on the surface Cr site (except for *n* = 4). For Ag₄Cr, the hydrogen molecule is adsorbed to a vertex Ag atom because its atomic coordination number (*N*_{Ag} = 2) is smaller than that of the surface Cr atom (*N*_{Cr} = 4). For *n* = 7–12, since the Cr dopant is encapsulated and coordination-saturated, the H₂ adsorption takes place on one of the surface host Ag atoms or on Ag–Ag bridging positions. The stable Ag_{*n*}Cr structures are preserved during the adsorption of H₂ either molecularly or dissociatively. Computed binding energies and second-order energy difference found Ag₃Cr–H₂/Ag₃Cr–2H and Ag₉Cr–H₂/Ag₉Cr–2H clusters relatively more stable, agreeing well with their high stability of bare counterparts. Importantly, dissociative H₂ adsorption is identified to be both thermodynamically and kinetically favorable for Ag₂Cr, Ag₃Cr, Ag₆Cr, and Ag₇Cr clusters. The molecular adsorption of H₂ on other Ag_{*n*}Cr species likely takes place over the dissociative one because of substantial energy barriers occurring during the dissociation (*n* = 4) or energetic preferences (*n* = 1, 5, and 8–12). Ag₃Cr, which is remarkably stable and barrierless during the reaction pathway, can serve as an efficient element for hydrogen dissociation and storage applications. Our finding results would provide a deeper understanding of the interaction of H₂ and Ag_{*n*}Cr clusters, including the adsorption site preference, the stability of adsorption configuration, the effect of impurity, plausible reaction pathways, and energy barriers involved as well as could offer informative guidelines for future experiments. This work contributes to the development of alloy clusters as elementary building blocks of novel nanostructured materials for hydrogen catalyst and storage applications.

ASSOCIATED CONTENT

Supporting Information

The Supporting Information is available free of charge at <https://pubs.acs.org/doi/10.1021/acsomega.2c04107>.

Structures of low-lying isomers of molecularly and dissociatively adsorbed H₂ on Ag_{*n*}Cr clusters (*n* = 1–12); partial and total DOS of thermodynamically preferred configurations for *n* = 4, 7, 8, and 10–12; and energy profiles (*n* = 4 and 7) as well as intrinsic reaction coordinates (4*n* = 2–4, 6, and 7) for dissociation of H₂ on Ag_{*n*}Cr clusters (PDF)

AUTHOR INFORMATION

Corresponding Authors

Nguyen Thi Mai – Institute of Materials Science and Graduate University of Science and Technology, Vietnam Academy of Science and Technology, Hanoi 11307, Vietnam; Email: maint@ims.vast.ac.vn

Nguyen Thanh Tung – Institute of Materials Science and Graduate University of Science and Technology, Vietnam Academy of Science and Technology, Hanoi 11307, Vietnam; orcid.org/0000-0003-0232-7261; Email: tungnt@ims.vast.ac.vn

Authors

Ngo Thi Lan – Institute of Materials Science and Graduate University of Science and Technology, Vietnam Academy of Science and Technology, Hanoi 11307, Vietnam; Institute of Science and Technology, TNU-University of Sciences, Thai Nguyen City 250000, Vietnam

Ngo Tuan Cuong – Center for Computational Science, Hanoi National University of Education, Hanoi 10000, Vietnam

Phung Thi Hong Van – Hanoi University of Natural Resources and Environment, Hanoi 10000, Vietnam

Duong Duc La – Institute of Chemistry and Materials, Hanoi 10000, Vietnam; orcid.org/0000-0003-4241-4431

Nguyen Minh Tam – Laboratory of Theoretical and Computational Biophysics, Advanced Institute of Materials Science, Ton Duc Thang University, Ho Chi Minh City 72915, Vietnam; Faculty of Pharmacy, Ton Duc Thang University, Ho Chi Minh City 72915, Vietnam

Son Tung Ngo – Laboratory of Theoretical and Computational Biophysics, Advanced Institute of Materials Science, Ton Duc Thang University, Ho Chi Minh City 72915, Vietnam; Faculty of Pharmacy, Ton Duc Thang University, Ho Chi Minh City 72915, Vietnam; orcid.org/0000-0003-1034-1768

Complete contact information is available at:

<https://pubs.acs.org/doi/10.1021/acsomega.2c04107>

Notes

The authors declare no competing financial interest.

ACKNOWLEDGMENTS

This work was supported by the Vietnam Academy of Science and Technology under grant no VAST03.03/21-22.

REFERENCES

- (1) Vanbuel, J.; Ferrari, P.; Janssens, E. Few-atom Cluster Model Systems for a Hydrogen Economy. *Adv. Phys.: X* **2020**, *5*, 1754132.
- (2) Dawson, J. K. Prospects for Hydrogen as an Energy Resource. *Nature* **1974**, *249*, 724.

- (3) Schlapbach, L.; Züttel, A. Hydrogen-storage Materials for Mobile Applications. *Nature* **2001**, *414*, 353.
- (4) van den Berg, A. W. C.; Aran, C. O. Materials for Hydrogen Storage: Current Research Trends and Perspectives. *Chem. Commun.* **2008**, 668.
- (5) Niaz, S.; Manzoor, T.; Pandith, A. H. Hydrogen Storage: Materials, Methods and Perspectives. *Renew. Sustain. Energy Rev.* **2015**, *50*, 457.
- (6) Fayet, P.; Kaldor, A.; Cox, D. M. Palladium Clusters: H₂, D₂, N₂, CH₄, CD₄, C₂H₄, and C₂H₆ Reactivity and D₂ Saturation Studies. *J. Chem. Phys.* **1990**, *92*, 254.
- (7) Nonose, S.; Sone, Y.; Onodera, K.; Sudo, S.; Kaya, K. Reactivity Study of Alloy Clusters Made of Aluminum and Some Transition Metals with Hydrogen. *Chem. Phys. Lett.* **1989**, *164*, 427.
- (8) Henry, D. J.; Yarovsky, I. Dissociative Adsorption of Hydrogen Molecule on Aluminum Clusters: Effect of Charge and Doping. *J. Phys. Chem. A* **2009**, *113*, 2565.
- (9) Wang, L.; Zhao, J.; Zhou, J.; Zhang, S. B.; Chen, Z. First-Principles Study of Molecular Hydrogen Dissociation on Doped Al₁₂X (X = B, Al, C, Si, P, Mg, and Ca) Clusters. *J. Comput. Chem.* **2009**, *30*, 2509.
- (10) Varano, A.; Henry, D. J.; Yarovsky, I. DFT Study of H₂ Adsorption on Magnesium-Doped Aluminum Clusters. *J. Phys. Chem. A* **2010**, *114*, 3602.
- (11) Lu, Q. L.; Wan, J. G. Sc-coated Si@Al₁₂ as High-capacity Hydrogen Storage Medium. *J. Chem. Phys.* **2010**, *132*, 224308.
- (12) Guo, L. First-Principles Study of Molecular Hydrogen Adsorption and Dissociation on Al_nCr (n = 1-13) Clusters. *J. Phys. Chem. A* **2013**, *117*, 3458.
- (13) Jia, M.; Vanbuel, J.; Ferrari, P.; Fernández, E. M.; Gewinner, S.; Schöllkopf, W.; Nguyen, M. T.; Fielicke, A.; Janssens, E. Size Dependent H₂ Adsorption on Al_nRh⁺ (n = 1-12) Clusters. *J. Phys. Chem. C* **2018**, *122*, 18247.
- (14) Jia, M.; Vanbuel, J.; Ferrari, P.; Schöllkopf, W.; Fielicke, A.; Nguyen, M. T.; Janssens, E. Hydrogen Adsorption and Dissociation on Al_nRh (n = 1 to 9) Clusters: Steric and Coordination Effects. *J. Phys. Chem. C* **2020**, *124*, 7624.
- (15) Kumar, T. J. D.; Tarakeshwar, P.; Balakrishnan, N. Geometric and Electronic Structures of Hydrogenated Transition Metal (Sc, Ti, Zr) Clusters. *Phys. Rev. B: Condens. Matter Mater. Phys.* **2009**, *79*, 205415.
- (16) Sheng, X.; Zhao, G.; Zhi, L. Evolution of Small Zr Clusters and Dissociative Chemisorption of H₂ on Zr Clusters. *J. Phys. Chem. C* **2008**, *112*, 17828.
- (17) Swart, L.; de Groot, F. M. F.; Weckhuysen, B. M.; Gruene, P.; Meijer, G.; Fielicke, A. H₂ Adsorption on 3d Transition Metal Clusters: A Combined Infrared Spectroscopy and Density Functional Study. *J. Phys. Chem. A* **2008**, *112*, 1139.
- (18) Trivedi, R.; Bandyopadhyay, D. Hydrogen Storage in Small Size Mg_nCo Clusters: A Density Functional Study. *Int. J. Hydrogen Energy* **2015**, *40*, 12727.
- (19) Trivedi, R.; Bandyopadhyay, D. Study of adsorption and dissociation pathway of H₂ molecule on Mg_nRh (n = 1-10) clusters: A first principle investigation. *Int. J. Hydrogen Energy* **2016**, *41*, 20113.
- (20) Charkin, O. P.; Maltsev, A. P. Density Functional Theory Modeling of Reactions of Addition of H₂ Molecules to Magnesium Clusters Mg₁₇M Doped with Atoms M of Transition 3d Elements. *J. Phys. Chem. A* **2021**, *125*, 2308.
- (21) Tai, T. B.; Nguyen, M. T. A three-dimensional aromatic B₆Li₈ complex as a high capacity hydrogen storage material. *Chem. Commun.* **2013**, 49, 913.
- (22) Tang, C. M.; Wang, Z. G.; Zhang, X.; Wen, N. H. The Hydrogen Storage Properties of Na Decorated Small Boron Cluster B₆Na₈. *Chem. Phys. Lett.* **2016**, *661*, 161.
- (23) Li, Y. C.; Zhou, G.; Li, J.; Gu, B. L.; Duan, W. H. Alkali-metal-doped B₈₀ as High-capacity Hydrogen Storage Media. *J. Phys. Chem. C* **2008**, *112*, 19268.
- (24) Li, M.; Li, Y. F.; Zhou, Z.; Shen, P. W.; Chen, Z. F. Ca-coated Boron Fullerenes and Nanotubes as Superior Hydrogen Storage Materials. *Nano Lett.* **2009**, *9*, 1944.
- (25) Li, J. L.; Hu, Z. S.; Yang, G. W. High-capacity Hydrogen Storage of Magnesium-decorated Boron Fullerene. *Chem. Phys.* **2012**, *392*, 16.
- (26) Wu, G. F.; Wang, J. L.; Zhang, X. Y.; Zhu, L. Y. Hydrogen Storage on Metal-coated B₈₀ Buckyballs with Density Functional Theory. *J. Phys. Chem. C* **2009**, *113*, 7052.
- (27) Dong, H.; Hou, T. J.; Lee, S. T.; Li, Y. Y. New Ti-decorated B₄₀ Fullerene as a Promising Hydrogen Storage Material. *Sci. Rep.* **2015**, *5*, 09952.
- (28) Bai, H.; Bai, B.; Zhang, L.; Huang, W.; Mu, Y.-W.; Zhai, H.-J.; Li, S.-D. Lithium-decorated Borospherene B₄₀: A Promising Hydrogen Storage Medium. *Sci. Rep.* **2016**, *6*, 35518.
- (29) Du, J.; Sun, X.; Zhang, L.; Zhang, C.; Jiang, G. Hydrogen Storage of Li₄B₃₆ Cluster. *Sci. Rep.* **2018**, *8*, 1940.
- (30) Lai, Q.; Paskevicius, M.; Sheppard, D. A.; Buckley, C. E.; Thornton, A. W.; Hill, M. R.; Gu, Q.; Mao, J.; Huang, Z.; Liu, H. K.; Guo, Z.; Banerjee, A.; Chakraborty, S.; Ahuja, R.; Aguey-Zinsou, K.-F. Hydrogen Storage Materials for Mobile and Stationary Applications: Current State of the Art. *ChemSusChem* **2015**, *8*, 2789.
- (31) Phala, N. S.; Klatt, G.; Steen, E. A DFT Study of Hydrogen and Carbon Monoxide Chemisorption onto Small Gold Clusters. *Chem. Phys. Lett.* **2004**, *395*, 33.
- (32) Buckart, S.; Ganteför, G.; Kim, Y. D.; Jena, P. Anomalous Behavior of Atomic Hydrogen Interacting with Gold Clusters. *J. Am. Chem. Soc.* **2003**, *125*, 14205.
- (33) Lang, S. M.; Bernhardt, T. M.; Barnett, R. N.; Yoon, B.; Landman, U. Hydrogen-promoted Oxygen Activation by Free Gold Cluster Cations. *J. Am. Chem. Soc.* **2009**, *131*, 8939.
- (34) Fang, Z.; Kuang, X. Hydrogen Molecule Adsorption on Au_nPt (n = 1-12) Clusters in Comparison with Corresponding Pure Au_{n+1} (n = 1-12) Clusters. *Phys. Status Solidi B* **2014**, *251*, 446.
- (35) Mondal, K.; Agrawal, S.; Manna, D.; Banerjee, A.; Ghanty, T. K. Effect of Hydrogen Atom Doping on the Structure and Electronic Properties of 20-Atom Gold Cluster. *J. Phys. Chem. C* **2016**, *120*, 18588.
- (36) Li, Y.; Li, Y.-F.; Tan, J.-J.; Jiang, B. F.; OuYang, Y.-Z. Probing Structure, Electronic Property, and Hydrogen Adsorption for Alkali Au_n Series. *Eur. Phys. J. Plus* **2017**, *132*, 159.
- (37) Lins, J. O. M. A.; Nascimento, M. A. C. A Density Functional Study of Some Silver Cluster Hydrides. *Chem. Phys. Lett.* **2004**, *391*, 9.
- (38) Zhao, S.; Liu, Z.-P.; Li, Z.-H.; Wang, W.-N.; Fan, K.-N. Density Functional Study of Small Neutral and Charged Silver Cluster Hydrides. *J. Phys. Chem. A* **2006**, *110*, 11537.
- (39) Manzoor, D.; Pal, S. Reactivity and Catalytic Activity of Hydrogen Atom Chemisorbed Silver Clusters. *J. Phys. Chem. A* **2015**, *119*, 6162.
- (40) Perera, S. M.; Hettiarachchi, S. R.; Hewage, J. W. Molecular Adsorption of H₂ on Small Neutral Silver-Copper Bimetallic Nanoparticles: A Search for Novel Hydrogen Storage Materials. *ACS Omega* **2022**, *7*, 2316.
- (41) Frisch, M. J. *Gaussian 09, Revision A02*; Gaussian, Inc.: Wallingford CT, 2009.
- (42) Hohenberg, P.; Kohn, W. Inhomogeneous Electron Gas. *Phys. Rev.* **1964**, *136*, B864.
- (43) Mai, N. T.; Lan, N. T.; Cuong, N. T.; Tam, N. M.; Ngo, S. T.; Phung, T. T.; Dang, N. V.; Tung, N. T. Systematic Investigation of the Structure, Stability, and Spin Magnetic Moment of CrM_n Clusters (M = Cu, Ag, Au, and n = 2-20) by DFT Calculations. *ACS Omega* **2021**, *6*, 20341.
- (44) Lan, N. T.; Mai, N. T.; La, D. D.; Tam, N. M.; Ngo, S. T.; Cuong, N. T.; Dang, N. V.; Phung, T. T.; Tung, N. T. DFT investigation of Au₉M nanoclusters (M = Sc-Ni): The magnetic superatomic behavior of Au₉Cr. *Chem. Phys. Lett.* **2022**, *793*, 139451.
- (45) Luo, Y. R. *Comprehensive Handbook of Chemical Bond Energies*; CRC Press: Boca Raton, FL, 2007.

(46) Tai, T. B.; Nguyen, M. T. A Stochastic Search for the Structures of Small Germanium Clusters and Their Anions: Enhanced Stability by Spherical Aromaticity of the Ge₁₀ and Ge₁₂ Systems. *J. Chem. Theor. Comput.* **2011**, *7*, 1119.

(47) Peng, C.; Ayala, P. Y.; Schlegel, H. B.; Frisch, M. J. Using Redundant Internal Coordinates to Optimize Equilibrium Geometries and Transition States. *J. Comput. Chem.* **1996**, *17*, 49.

(48) Gonzalez, C.; Schlegel, H. B. Reaction Path Following in Mass-weighted Internal Coordinates. *J. Phys. Chem.* **1990**, *94*, 5523.

(49) [Supporting Information](#).

(50) Kleis, J.; Greeley, J.; Romero, N. A.; Morozov, V. A.; Falsig, H.; Larsen, A. H.; Lu, J.; Mortensen, J. J.; Dulak, M.; Thygesen, K. S.; Norskov, J. K.; Jacobsen, K. W. Finite Size Effects in Chemical Bonding: from Small Clusters to Solids. *Catal. Lett.* **2011**, *141*, 1067.